



McGill
MACDONALD CAMPUS

**McGill University, Faculty of Agricultural and Environmental
Sciences, Department of Bioresource Engineering**

Student-Designed Solar Water Heating System for McGill Student Residences



Bennett, Laurie

Brière-Deschênes, Marilyn

Glover, Antony

Konrad, Mary Elizabeth

January 2013 – April 2013

EXECUTIVE SUMMARY

The following report summarizes the second and final phase of a design project aimed at examining alternative hot water heating systems for the Upper Residences of McGill University during summer when occupancy decreases to less than half of full capacity. Phase one resulted in the recommendation of a roof-mounted solar thermal system with an air source heat pump to supplement demand during periods of high demand and poor insolation. Phase two includes in-depth engineering analysis of roof fixation methods and roof load capacity requirements based on wind and snow loads. Design drawings show a potential configuration of collectors on the roof. System diagrams outline all components required, their specifications, and how they are integrated into the system. A computational model was developed which confirmed the effectiveness of the primary and supplementary systems in three critical insolation and demand scenarios and established that glycol pipe insulation inside the building can effectively eliminate heat losses in the pipes. Lastly, system failure modes and risks are discussed, and general system recommendations for the client are provided.

REMARKS

This report is intended for internal use only as some figures may constitute copyright infringement. Figures were used to facilitate the comprehension of concepts and have been used purely for educational purposes as part of the BREE Senior Design course. A review of ownership rights should be performed before any publication of this document. No copyright infringement was intended.

ACKNOWLEDGEMENTS

McGill Energy project

Marc-Etienne Brunet, Coordinator, energyproject@mcgill.ca

McGill Residences Buildings and Facilities Operations

Tatjana Trebic, Project Coordinator, tatjana.trebic@mcgill.ca

David Balcombe, Associate Director

Robert Patterson, Maintenance Technician

Jonathan Rousham, Maintenance Manager

McGill University, Bioresource Department

Dr. Grant Clark, course supervisor, grant.clark@mcgill.ca

Janick Hardy, Collaborator in the Design II project

Jason Ng Cheng Hin, Masters Student at McGill

We would like to express our gratitude towards all those who have been involved in the development of the McGill Energy Project. It is a collaboration of students, faculty, and staff working towards energy sustainability on campus through applied research. The project aims to tackle the university's energy usage, to create a unique collaborative learning experience for everyone involved, and to foster the next generation of energy leaders.

Through this organization, our team was able to take on a challenging project to benefit our local community, to communicate with multiple mentors within the McGill staff and student body and to access essential information that would otherwise be impossible to obtain as independent students. Their contribution to our learning experience has been invaluable.

For more information about the McGill Energy Project, please contact energyproject@mcgill.ca or visit their Facebook page.

CONTENTS

Executive Summary	2
Remarks	2
Acknowledgements.....	3
List of Figures.....	7
List of Tables	8
1. Design 2 project: feasibility assessment	9
1.1 Context and Objectives	9
1.2 Results.....	9
2. Design 3 Overview	11
2.1 Objectives.....	11
2.2 Competition entered	11
3. Engineering Analysis and Design Specifications	13
3.1 Collector Load Analysis and Installation Methods	13
3.1.1 Snow Load	13
3.1.2 Wind Load	14
3.1.3 Friction Calculations.....	17
3.1.4 Overturning moment.....	18
3.2 Rooftop Collector Configuration	19
3.2.1 Collector Orientation and Design.....	19
3.3 System ComponentS	25

3.31	Solar Collectors	26
3.32	Heat pump.....	26
3.33	Water Storage Tank & Heat exchanger	27
3.34	Differential Controllers/Temperature sensors	28
3.35	Expansion tank	28
3.36	Glycol pump	29
3.37	Glycol Pipes.....	31
3.38	Other components.....	32
4.	Computational System Model.....	33
4.1	Description of the Model.....	33
4.1.1	Purpose	33
4.1.2	Concept.....	33
4.1.2.2	Glycol Pipes (Block 2)	35
4.1.2.3	Storage Tank and Heat Exchanger (Block 3)	35
4.1.2.4	Initial Conditions and Limits	36
4.3	Results	36
4.3.1	Validation of Selected Parameters.....	37
4.3.2	Comparison of Insulated and Non-insulated Pipes.....	38
4.3.3	Sizing the Heat Pump	39
5.	Risk and failure Analysis	41
5.1	Model Reaction to Extreme Scenarios	41

5.2 Component Failure	41
5.3 Rooftop Concerns.....	42
5.4 Economics of Risk	43
6. optimization & Recommendations	44
6.1 Roof Considerations.....	44
6.2 System Components.....	44
6.3 The computational Model	45
Final Remarks	46
References.....	47
Appendix.....	50
Appendix A – Roof Load.....	50
Appendix B: Comparison of tilt angles for solar collectors.....	52
Appendix C: Collector Efficiencies	53
Appendix D: System Components	54
Appendix E: Computational Model	57

LIST OF FIGURES

Figure 1: Aerial view of McGill Upper Residences	9
Figure 2 - Results of feasibility assessment	9
Figure 3: Free body diagram of wind loads on a collector	16
Figure 4: Sunpath diagram for Montreal (Gaisma).....	20
Figure 5: Collectors configuration - reverse return piping (Kalogiro, 2009)	21
Figure 6:Collector configuration (AEE , 2009)	22
Figure 7: Plan view of roof layout of one of Molson Hall for configuration of maximum number of thermal collectors (3m between rows).....	23
Figure 8: Three-dimensional view of Molson Hall from the East	24
Figure 9: Front South-East view of Molson Hall.....	24
Figure 10: South view of Molson Hall	25
Figure 11: Comparison of pumping requirement for corn and ethylene glycols as a function of temperature	31
Figure 12: System component diagram	32
Figure 13: Diagram of the computational model broken down into 3 main blocks	34
Figure 14: Accumulated Heat Loss (deg. C) in non-insulated glycol pipes over 72 hours	39
Figure 15: Accumulated Heat Loss (deg. C) in insulated glycol pipes over 72 hours	39
Figure 16: Results of simulation with best (yellow), medium (violet) and worst-case (blue) scenarios show tank temperature (deg. C) over time (hrs)	40
Figure 17: Comparison of Panel Efficiencies (Calpak)	53
Figure 18 - Simplified schematic of piping distances on the roof	55

Figure 19: Scenarios for computer model simulations 59

LIST OF TABLES

Table 1: Summary of wind load results 16

Table 2: Summary of friction calculation results..... 18

Table 3: Summary of moment analysis 19

Table 4: Dimensions of main components..... 26

Table 5: Average irradiance data for Montreal (RETScreen)..... 37

Table 6: Parameters used to calculate head loss throughout the glycol loop, based on both main glycol pipes and pipes in collectors 54

1. DESIGN 2 PROJECT: FEASIBILITY ASSESSMENT

1.1 CONTEXT AND OBJECTIVES

McGill's three Upper Residences, shown in Figure 1, currently use district steam production for water and space heating. From roughly April 30 to October 1, the steam pipes for space heating are shut down, while those required to heat water remain open. The system as a whole must therefore be kept running for 4 months of the year during which occupancy is generally near-zero.

Research has indicated that this incurs an annual cost of \$ 13 000 per building (Parr, Feb 2012).



Figure 1: Aerial view of McGill Upper Residences

Prompted by these findings, in September 2012, the MEP and McGill Buildings and Facilities Operations approached this student group with a proposed project: to select and design a system that would allow all steam pipes to be shut down during the summer months, while providing hot water to building occupants at a potential 50% occupancy. Based on Bioresource Engineering Design 2 and 3 guidelines, the fall semester would involve a feasibility assessment, followed by further design of the selected alternative system in the winter semester.

1.2 RESULTS

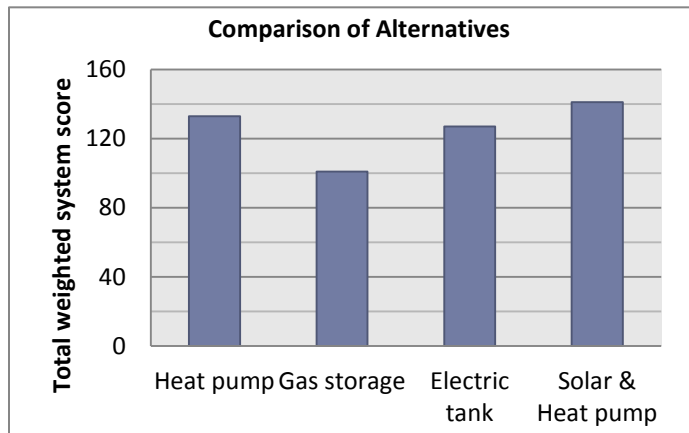


Figure 2 - Results of feasibility assessment

The most viable potential heating systems, shown in **Erreur ! Source du renvoi introuvable.** were compared using a set of criteria and weightings, which can be found in the Design II report. Based on these criteria, the solar thermal system was selected for further design in the winter semester. Though

the heat pump obtained similar results and requires less complex installation and maintenance, it was dismissed as the solar thermal alternative provides an opportunity for innovative design. This final decision was made by the student team as well as the MEP and the client at a meeting in December.

2. DESIGN 3 OVERVIEW

2.1 OBJECTIVES

According to the course guidelines for Design 2 and Design 3, the student final design project should progress in a cycle that begins with problem definition, synthesis of information, evaluation of possible solutions and selection of a best solution at the end of Design 2. It then follows these steps with the four other steps of the engineering design cycle, which represent the essence of Design 3. First, an analysis and calculations must be done to specify a system customized to the client. The following step is to either build a prototype or model the system. Then, tests and evaluations should be run to assess risk, failure modes and other potential weak points of the design. Based on this information, students are then expected to optimize and revise the final design.

In the context of the Design 3 part of this particular project, the primary objective was to design a more detailed solar thermal water heating system for one of the Upper Residence buildings as an alternative to the current steam system used for heating water during the summer months. The design should be made primarily for 50% full occupancy in order to meet potential demand during the months of May to August. However, the system could also be used year round in order to supplement or preheat the steam system during normal student occupancy months (September to April). In particular, this part of the project is meant to identify the implications, limitations and full potential of a custom-designed solar thermal water heating system in the McGill residences, in order to develop a complete design recommendation for potential implementation.

2.2 COMPETITION ENTERED

In conjunction with the MEP, the members of our design team submitted this project as a candidate for the 2013 Scotia Bank EcoLiving Awards. Out of the three possible categories, it was submitted in the \$10,000 Student Leadership Award category, for the post-secondary students with an innovative concept or prototype aimed at energy conservation. The finalists for

these awards should be announced in May 2013. More details can be found on the competition's website (<http://ecoliving.scotiabank.com/awards>).

3. ENGINEERING ANALYSIS AND DESIGN SPECIFICATIONS

3.1 COLLECTOR LOAD ANALYSIS AND INSTALLATION METHODS

3.1.1 SNOW LOAD

To ensure that the roof load capacity is sufficient to support the extra weight of the solar collectors, the load caused by snow accumulation must be determined and subtracted from the total roof load capacity. The following equation from the 2010 National Building Code of Canada was used to calculate the snow load on the residence roofs. Refer to Appendix A for a more detailed explanation of the how the I_f and C_b factors were determined.

$$S = I_f * (S_s(C_b C_w C_s C_a) + S_r) \quad (1)$$

Where,

$$I_f = 1.15 \text{ high importance (school residence)}$$

$$S_s = 2.6 \text{ kPa (Montreal, City Hall)}$$

$$C_b = 0.8 (L_c \text{ less than } 70\text{m, see Appendix A})$$

$$C_w = 1.0 \text{ high importance}$$

$$C_s = 1.0 \text{ (slope less than or equal to } 30 \text{ degrees)}$$

$$C_a = 1.0 \text{ (for a flat roof)}$$

$$S_r = 0.4 \text{ kPa (Montreal, City Hall)}$$

$$S = 1.15 * ((2.6 * 0.8 * 1 * 1 * 1) + 0.4)$$

$$S = 2.825 \text{ kPa}$$

Thus the maximum anticipated snow load is 2.8 kPa.

3.1.2 WIND LOAD

The client would like to avoid puncturing the roof membrane and potentially causing roof leaks. Thus, it is preferred that a system of ballasts be used to keep the collectors in place. In order to determine how many collectors the roof can hold, we must consider both the space available, and the load capacity of the roof. The required ballast weight must be determined using wind data for the site to calculate the vertical forces, horizontal forces and turning moments that will be exerted by the wind on collectors of a given geometry and mounting angle. Typically, the required ballast weight is found using data collected in wind tunnel simulations performed by the company producing the collectors and mounting system. This method is impractical for an unfunded preliminary design recommendation. Rather, a simplified, conservative calculation will be used to evaluate the practicality of using a ballast system to fix collectors to the roof at the proposed angles of 19 and 69 degrees. The values generated should be compared to the roof load capacity when such a value is obtained. Wind pressures from the National Building Code of Canada will be used in the following equation for fluid pressure on a wall perpendicular to the incident flow.

$$p = \frac{1}{2}\rho v^2 \quad (2)$$

Where,

$$\rho = \text{air density (kg/m}^3\text{)}$$

$$v = \text{wind velocity (m/s)}$$

In our case, $\frac{1}{2}\rho v^2 = q$ where q is the 1/30 year hourly wind pressure provided by the National Building Code of Canada for Montreal, Quebec. The 1/30 year value has been selected since the lifespan of the system is approximately 25 years. The q value is multiplied by two because the pressure acts both on the windward side, and on the leeward side of the collector (dead-air suction). Typically, this value would instead be multiplied by a lift or drag coefficient derived from the angle of the panel and projected area. However, such coefficients are difficult to

determine for high angles such as 69 degrees. A coefficient of 2 is used as a conservative estimate.

The pressure is then adjusted for the angle of the panel in each calculation using trigonometric ratios. Then this pressure (normal to the collector face) is converted to an equivalent point force acting at the centre of the panel, by multiplying by the collector surface area. The equation below summarizes these conversions.

$$F_N = 2 q \cos(90 - \theta) \quad (3)$$

Where,

$\theta = \text{panel tilt angle}$

$F_N = \text{equivalent point force normal to the collector surface}$

Figure 3 shows a free body diagram of the forces acting on the collectors in each of two cases: a Northerly wind, and a Southerly wind. The light coloured arrows represent the evenly distributed wind pressure q , and the dark arrows represent the resultant equivalent point forces (F_N) normal to the collector surface which were found.

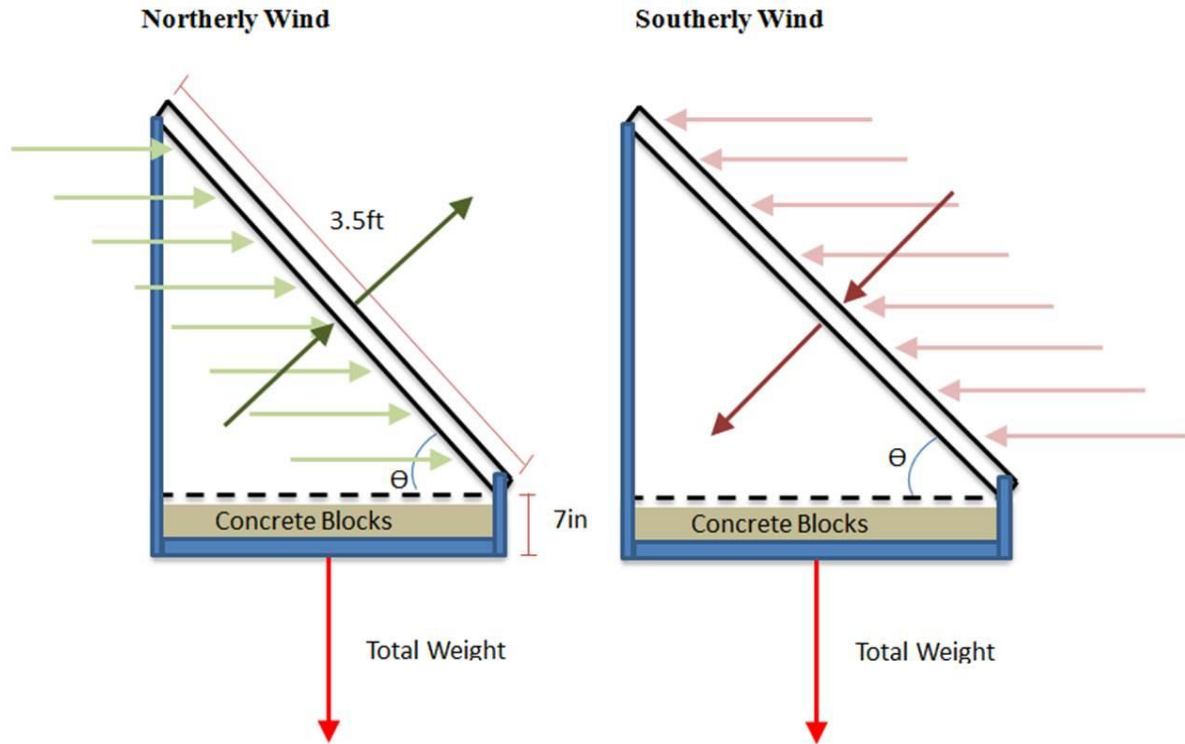


Figure 3: Free body diagram of wind loads on a collector

The point forces were decomposed into their vertical and horizontal components. Table 1: Summary of wind load results is a summary of the resulting values. See attached Excel spreadsheet for detailed calculations and formulas.

Table 1: Summary of wind load results

Angle (deg)	Wind	q (kPa)	q normal (kPa)	Normal Point Force (kN)	Vertical Force (N)	Horizontal Force (N)	Spatial Direction
19	Southerly	0.37	0.24	0.60	570.34	196.38	down and north
19	Northerly	0.37	-0.24	-0.60	-570.34	-196.38	up and south
69	Southerly	0.37	0.69	1.73	619.87	1614.82	down and north
69	Northerly	0.370	-0.691	-1.730	-619.871	-1614.819	up and south

The Southerly wind case has a positive vertical force meaning that a force is acting in the downward direction, thus it is the case which imposes the maximum load on the roof. The Northerly wind has a negative vertical force, implying lift, and requiring the addition of ballast weight to counteract this force and prevent lift-off. Sliding is also a concern that is addressed in the following section.

3.1.3 FRICTION CALCULATIONS

The friction between the ballast trays and the roofing material must also be taken into account to avoid sliding. The friction force generated must exceed that of the drag force exerted by the wind in order to avoid sliding of the collectors. The friction force in question is static friction since we do not want to allow the collectors to ever start to slide (dynamic friction). The formula for static friction is the following:

$$F_f = \mu_s F_V \quad (4)$$

Where,

F_f = *the static friction force*

μ_s = *the coefficient of friction between the two materials*

F_V = *the force normal to and toward the friction surface*

We will assume a coefficient of friction of 0.4 for rubber roofing against stainless steel ballast trays (Viridian Solar, 2013). Table 2 includes the results for the total ballast required to resist lift and sliding at both collector angles. The roof must be able to support the total load applied to the roof when using the larger of the ballast values in order for a multi-angle system to be safely implemented. See attached Excel spreadsheet for detailed calculations and formulas.

Table 2: Summary of friction calculation results

Angle (degrees)	Wind	Net F _v	Friction force	Sliding?	Force lacking	Required ballast kg	Max roof load kg/collector
19	Southerly	951.81	380.72	no	-215.37	0.00	97.02
19	Northerly	-188.87	-75.55	yes	925.31	94.32	133.21
69	Southerly	1001.34	400.54	yes	5054.23	515.21	617.29
69	Northerly	-238.40	-95.36	yes	6293.97	641.59	680.47

The equivalent pressure of the maximum load at 69 degrees is 2.8 kPa (similar to that of the snow load) while the maximum pressure at 19 degrees is 0.4 kPa if only enough ballast is applied for that angle. Thus if, upon further examination, 2.8kPa is too heavy for the roof capacity, a smaller angle, or a year-round angle of 19 degrees could be used to drastically reduce the load on the roof.

It is assumed that, by applying adequate ballast to prevent sliding, and multiplying by a safety factor of 1.5, winds coming from angles other due North and due South will not be able to cause unwanted panel rotation.

3.1.4 OVERTURNING MOMENT

It is also important to determine whether the wind could cause a moment which would result in the overturning of the panels. This is calculated by doing a force balance of the moments acting on the panel, assuming the pressure on the collector can be treated as a point load at the centre of the collector. The ballast will be uniformly distributed over the maximum projected area of the panel on the roof (this occurs when the angle is set at 19 degrees), and modeled as a point load at a distance of ½ the projected horizontal length of the panel from the point of rotation. Since the moment increases with the length of the moment arm, the ballast required to resist overturning may be minimized by minimizing the moment arms. Thus, it is advantageous to orient the collectors with the long axis in the horizontal direction. This will also make the panels less noticeable from the ground which may be more aesthetically pleasing and thus advantageous for receiving approval from regulatory bodies such as the Mount-Royal Friends of the Mountain.

We will assume there is a 7 inch vertical gap between the bottom edge of the collector and turning point of the panel. This will accommodate 3 layers of 2 inch thick solid concrete slabs, if needed. Using heavy concrete blocks with a density of 125 lb/ft³ (Boral, 2013), the volume of concrete in a 6 inch layer which fits under the 3.5ft x 7.7 ft footprint of our collectors, when set at a 19 degree tilt, would provide 724 kg of ballast. This is more than enough for the 642 kg required for the worst-case wind load scenario analyzed above.

The moments calculated are for the maximum horizontal force (full wind scenario) with the minimum vertical load (Northerly wind causing lift) since this is the most critical scenario which could result in overturning. The moment arms for each of the point wind loads in each scenario are 1/2 the projected vertical height of the collectors at the given angle, plus 7 inches. The moment arm of the vertical load is assumed to be at the centre of the ballast tray in both scenarios (half of the projected length of the tray). Table 3 shows the result of the tipping calculations.

Table 3: Summary of moment analysis

Collector Angle (degrees)	Moment arm of horizontal force (m)	Max horizontal force (N)	Net vertical force @max horizontal force (N)	Moment arm of vertical force (m)	Moment CCW (Nm)	Moment CW (Nm)	Tipping?
19.00	0.35	196.38	381.47	0.50	69.02	192.39	NO
69.00	0.68	1614.80	5435.70	0.50	1091.24	2741.44	NO

Tipping will not occur in design wind conditions at either collector angle since the moment generated by the vertical downward forces (called Moment CW) exceed that of the horizontal wind forces in the worst case scenarios.

3.2 ROOFTOP COLLECTOR CONFIGURATION

3.2.1 COLLECTOR ORIENTATION AND DESIGN

The collectors should always face the equator for maximum efficiency, meaning that collectors in the Northern hemisphere should face South and collectors in the Southern hemisphere should face North. In addition, the tilt angle of a collector also affects its efficiency. In the case of a

fixed system of flat plate collectors (no solar tracking), the tilt angle is a very important factor. In the summer, the sun is high in the sky whereas in the winter, the sun is at a much lower angle, as illustrated in Figure 4: Sunpath diagram for Montreal (Gaisma). For a system

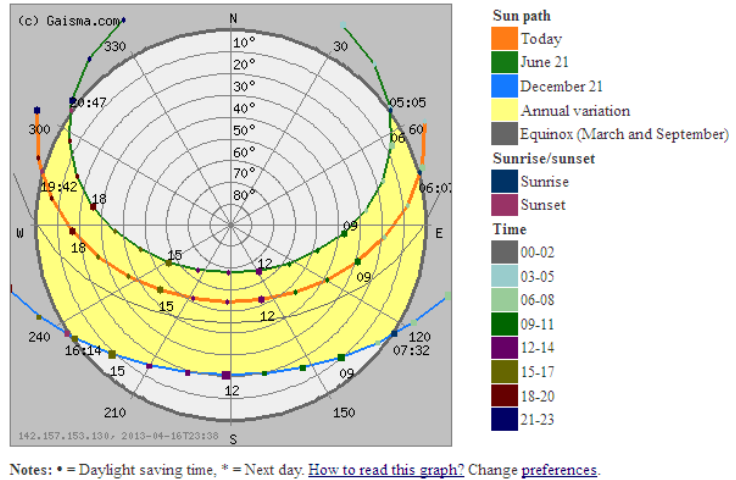


Figure 4: Sunpath diagram for Montreal (Gaisma)

that will be used year-round, it is recommended that the angle of tilt be equal to the degrees of latitude of the location (AEE , 2009). However, in the particular case of the McGill residences, since most of the system usage will occur during the summer months and the system will only meet part of the full student occupation demand, the collector angle should be optimized primarily for summer operation. An angle of 19 degrees would be the optimal tilt for summer and 69 degrees would be optimal for winter according to the location of the residences. Additionally, a steeper angle is beneficial in winter, as it eliminates snow accumulation on collectors. According to the National Building Code of Canada, with a tilt angle of more than 60 degrees on a smooth surface, no snow will accumulate. Appendix B contains a table of the resulting seasonal efficiencies of collectors according to tilt angle. In this table, a tilt angle of 19 degrees is recommended for April to September and a tilt angle of 69 degrees from October to March.

The typical size of a solar collector is 4ft x 8ft or approximately 3m² (Alternative Energy Tutorials, 2012). They are usually combined in modules, which are positioned in series. A maximum of 80-100m² of collectors can be connected in series (AEE , 2009). In this case, the dimensions of the chosen 240GA collector model from the company Calpak vary slightly from this norm (Calpak Solar Thermal). The chosen panels measure 3.5 feet by 7.7 feet (1.067m by 2.347m), resulting in a collector area of 26.95 feet² (2.50m²). In this study for the McGill residences, 5 modules would be connected in parallel, each made up of 12 collectors connected in series. A rough schematic of this panel configuration is provided in Figure 5: Collectors

configuration - reverse return piping (Kalogiro, 2009). The total collector area results to 150m^2 . Typically, a collector area of 1.1m^2 to 1.3m^2 per person is required in the northern United States (US Department of Energy, 2003). Designing for 50% occupancy capacity (~ 100 people) and assuming the largest parameters, according to the reference in the previous sentence, an area of 150m^2 should be sufficient to supply the energy needed, which equates to 60 collectors needed for our design of this project.

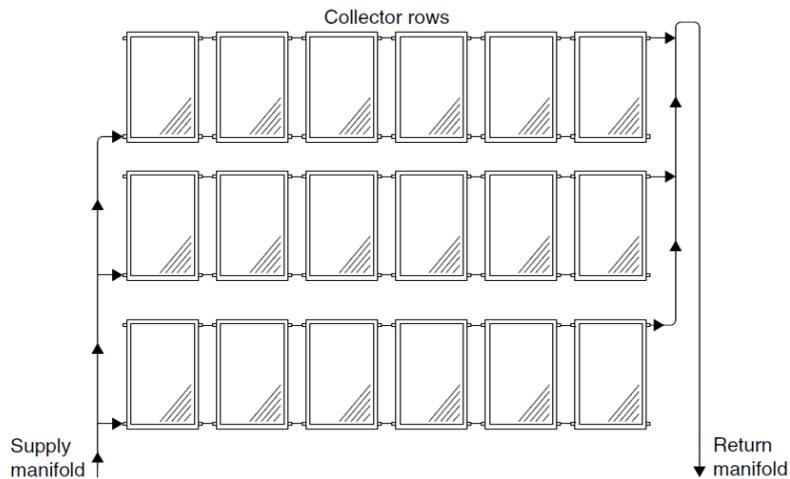


Figure 5: Collectors configuration - reverse return piping (Kalogiro, 2009)

When multiple collectors are installed on the roof, there is a risk that they will shade each other as shown in Figure 6, which would decrease their efficiency. A simple calculation can be done in order to approximate the minimum distance required between each row to eliminate shading, as shown in Figure 6 and Equation (5) (AEE , 2009).

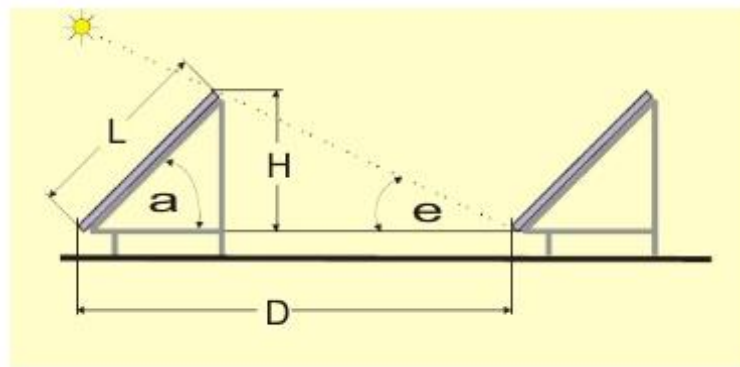


Figure 6: Collector configuration (AEE , 2009)

$$D = \frac{L \sin[180 - (\alpha + \epsilon)]}{\sin \epsilon} \quad (5)$$

Where

D = Distance between the rows of collectors (m)

ϵ = Incident solar minimum radiation angle (21,1 degrees)

α = Collector inclination (69 degrees)

L = Collector length (1.0668 m)

The time at which shade reach its maximum is when the sun is at its lowest point in the sky, occurring on December 21st (Time and date, 2012). According to the previous calculations, the distance between the rows should be 2.98 m which can be approximated to 3.00 m. This is represented by distance D in Figure 6:Collector configuration

Therefore, we can approximate the area of the roof required per collector. Knowing that the distance needed between collector rows is 3 m and the collector width is 2.347 m, 7.04 m² of roof area required per collector. With 58 panels, an available area of approximately 408.3 m² is necessary in order to eliminate shading.

However, even though the available roof space is approximately 744m², there are further considerations to address for proper collector configuration. To begin, as seen in Figure 8, there is an additional floor located in the center of the roof, occupying part of the main roof.

Theoretically panels could be placed atop this center part, but for practical reasons we shall limit the installation of collectors to the main roof area. Continuing on, since the collectors need to be oriented toward the South, this further complicates the required roof area for the collectors. In order to visualize the space that collectors would take up, a diagram was generated, since calculations were not suited to the problem.

Below is a plan view of the selected collector configuration for the roof layout. The building shown is Molson Hall; it was chosen for potential implementation because, of the three Upper

Residences, it has the most recently renovated roof. Collectors were placed wherever possible on the main roof level area to evaluate the maximum number of collectors that could fit based on the constraints established above. Given this configuration, a maximum of 69 panels with the dimensions corresponding to the chosen panel model (3.5 ft by 7.7 ft) were able to be placed on the roof. Please keep in mind that this number represents the maximum only when collector configuration is designed to eliminate shading in the worst-case scenario: lowest angle of sun in winter solstice (21 degrees) and collector tilt at highest angle (69 degrees). If a different collector angle was chosen, this would reduce the amount of space needed between rows. This will be discussed in more detail in the optimization section.

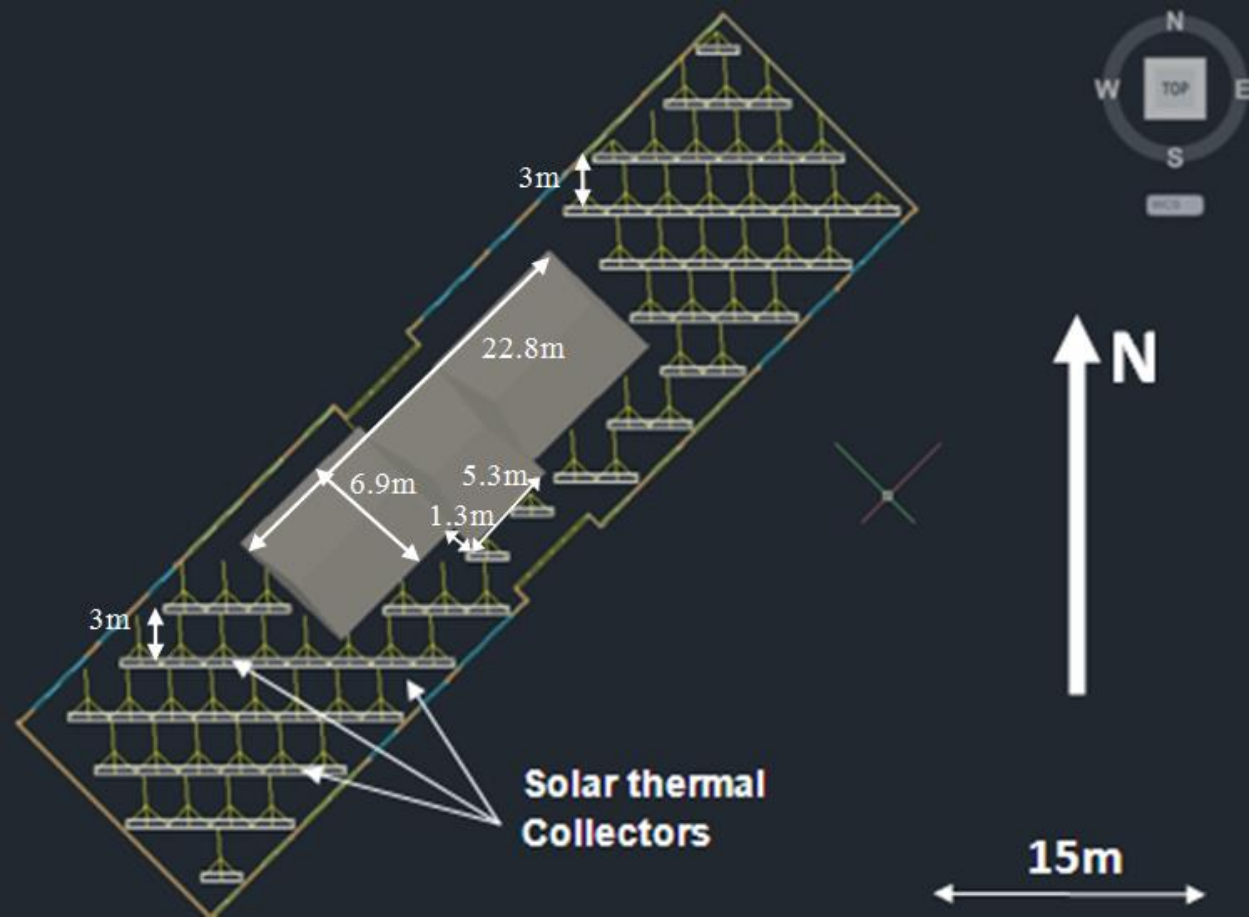


Figure 7: Plan view of roof layout of one of Molson Hall, for configuration of maximum number of thermal collectors (3m between rows)

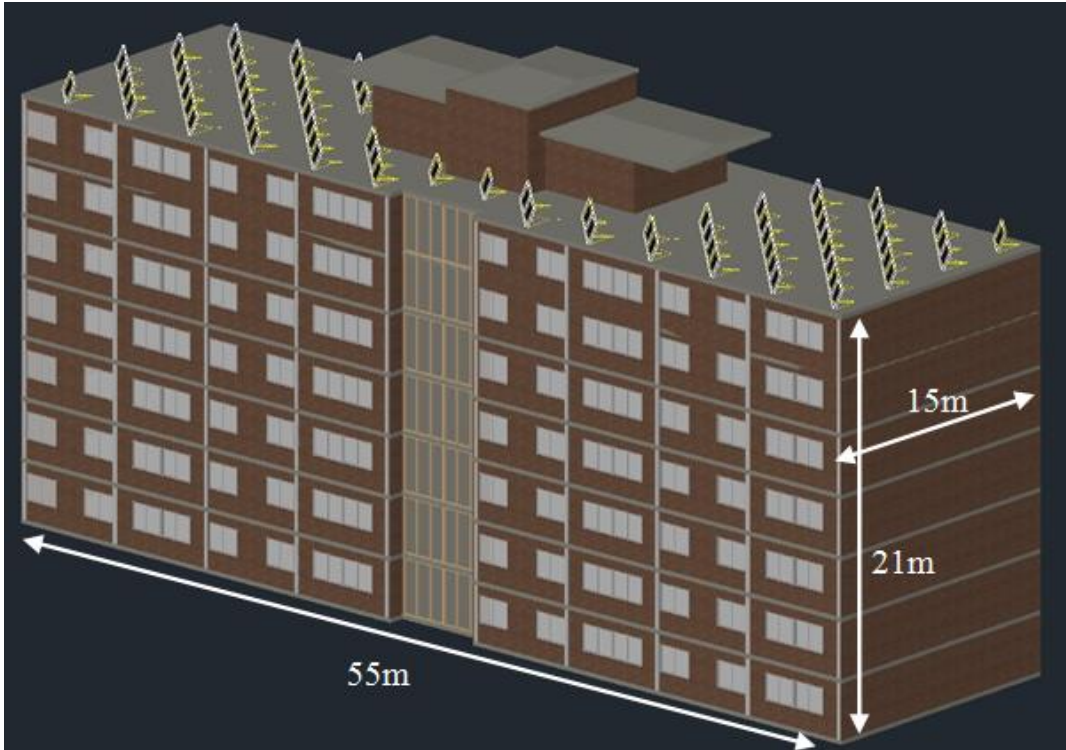


Figure 8: Three-dimensional view of Molson Hall from the East



Figure 9: Front South-East view of Molson Hall

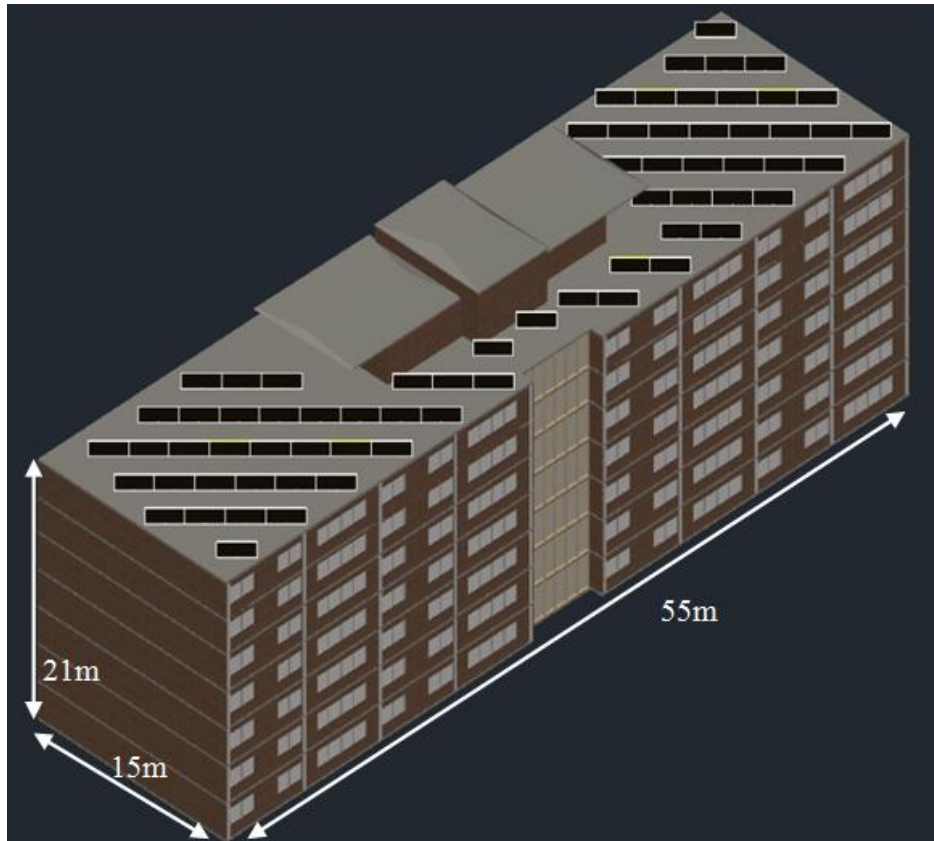


Figure 10: South view of Molson Hall

3.3 SYSTEM COMPONENTS

A solar water heating system requires numerous key components that can be configured in many ways. Components include solar collectors, tanks, a heat exchanger, a glycol pump, the heat pump, and a glycol expansion tank. After a visit to the Molson Hall basement, we were able to develop a better idea of the available space in the mechanical room. Dimensions of components to be installed in the basement are listed in Table 4. Other components must also be taken into consideration, such as valves, temperature sensors and controllers, air elimination systems, pressure gauges, piping and fittings. The calculations in the following section have been based on the recommendations of solar heating companies operating in Quebec, as well as plumbing companies that specialize in solar thermal systems (EcoSolaris, 2013).

Table 4: Dimensions of main components

	Volume (ga)	Length	Width/diameter	Height
Atmospheric tank (Aps, 2004)	750		48	72
Storage tank (AO Smith, 2012)	1,500	107	66	
Heat pump	422	63	38	43
Expansion tank (Cash Acme, 2006)	100		23.38	59

*dimensions are in inches

3.31 SOLAR COLLECTORS

For our climate, flat plate collectors are most suitable, as they are more durable in the long-term. Though evacuated tubes might be more efficient, they are more prone to damage (EcoSolaris, 2013). Calpak Solar Thermal in Bristol, Connecticut carries two models of flat plate collector: the 240GA and 240G. The GA series panel has an aluminum collector plate, thus it weighs significantly less than the G series model which has a collector plate made of two sandwiched stainless steel plates. The two models weigh 84 and 134 lbs respectively (38.1kg and 60.8kg). The lighter of the two models has been chosen, since it has a much higher efficiency in cooler climates such as Montreal's (CalPak Solar Thermal, 2008). The comparative efficiency graph for the different models can be found in Appendix C.

Further specifications for the chosen collectors are addressed in Section 3.2.

3.32 HEAT PUMP

Based on our comparison from last semester, a heat pump is the most efficient technology to supplement the solar water heating system when the solar conditions are not optimal. It displaces heat as a refrigerator would instead of creating it and is therefore a more efficient energy source than conventional electric water heaters (See Design 2 report).

3.33 WATER STORAGE TANK & HEAT EXCHANGER

An essential component of the system is a storage tank. There are two types: pressurized and atmospheric. The first can withstand city water pressure without rupturing since pressure relief valves have to be included in their design. If the pressure builds up too high inside the tank, the relief valve opens and water is released. The tanks must also be insulated to minimize heat loss.

Atmospheric tanks are non-pressurized containers. These are not always completely sealed and, as such, they will allow evaporation and should be well insulated. They are cheaper than pressurized tanks and are recommended for economic reasons when tank capacity must exceed 240 gallons. They also require less maintenance than pressurized tanks since they do not contain anode rods, which would need to be changed regularly (Solar Hot USA, 2009). Given that the volume of water to be stored in the residences is significant, the possibility of using atmospheric tanks should be investigated in order to minimize costs.

An atmospheric tank with two coils for heat transfer is a good option. One coil, at the bottom of the tank, is for the glycol loop that runs all the way to the solar collectors. The other, in the top section of the tank, is for the water that will be heated and then stored in a larger pressurized tank. This has been recommended since the water in the atmospheric tank does not circulate and thus allows thermal stratification to occur when placed in a vertical position. The atmospheric tank, once filled with water, is closed and sealed to avoid evaporation. The water contained in the atmospheric tank should be changed every 6 to 7 years, but such tanks have a life span of 20 to 25 years as their design limits corrosion (EcoSolaris, 2013).

For efficient heat transfer, a heat exchanger needs 0.2 m² of surface area per m² of collector (UK Copper Board, 2010).

$$A_{coil} = 144 \text{ m}^2 * 0.2 \text{ m}^2/\text{m}^2 \text{ of collectors} = 28.8 \text{ m}^2$$

$$\text{For 1" type L of coil diameter: Circumference} = 0.07979 \text{ m}$$

$$\text{Length of coil needed} = 28.8 \text{ m}^2 / 0.07979 \text{ m} = 360.9 \text{ m}$$

$$V_{coil} = 360.9 \text{ m} * (\pi (0.0254 \text{ m}/1\text{in})^2) = 0.7315 \text{ m}^3$$

$$2 \text{ coils of } 0.7315 \text{ m}^3 = 1.463 \text{ m}^3 = 387 \text{ gallons}$$

The atmospheric tank should be 750 gallons to allow a proper heat exchange, as it should have a volume that is at approximately double the total outer volume of the heat exchange coils. A pressurized storage tank for water is also needed to complete the system. This tank will contain water that has been heated by the upper coil of the heat exchanger. The volume of a storage tank should be equal to the daily consumption in hot water (UK Copper Board, 2010).

$$\text{Consumption} = 52 \text{ L/day/person} * 110 \text{ person} = 5720 \text{ L/day}$$

$$V_{\text{tank}} = 1511.06 \text{ gallons} = 5.72 \text{ m}^3$$

According to calculations above, the storage tank has been selected to hold 5720 L (1,500 gallons) of hot water.

3.34 DIFFERENTIAL CONTROLLERS/TEMPERATURE SENSORS

Two temperature sensors are required: the first, where the glycol exits the panels on the roof and the second, at the bottom of the atmospheric tank/heat exchanger. The temperature difference between the two sensors will send information to the controller which will regulate the flow rate of the glycol pump. When the solar energy is high and the glycol temperature is greater than the temperature at the bottom of the atmospheric tank and the glycol will be pumped at a faster rate. Under cloudy conditions, the temperature differential between the roof and tank will be smaller, thus the glycol will circulate at a slower flow rate in order to acquire the same amount of energy. In the worst possible conditions, if the temperature of the glycol on the roof is less than the water in the atmospheric tank, the pump should stop running to avoid a situation where the glycol would cool the water.

3.35 EXPANSION TANK

An expansion tank is needed to control the thermal expansion of the glycol. The pressure resulting from the expansion of the heat transfer fluid as it heats up may cause the relief valve to discharge to avoid unsafe conditions. The expansion tank has to have a minimum volume of 100 gallons according to the Bosch's solar thermal expansion tank sizing guide (Bosch, 2011).

Volume of Expansion tank:

$$V_{\text{expansion tank}} = \frac{(V_{\text{exp}} + V_{\text{vap exp}}) \times (P_{\text{sv}} + 14.5 \text{ psi})}{(P_{\text{sv}} - P_{\text{initial}})} \quad (6)$$

$$V_{\text{collectors}} = 0.000743 \text{ m}^3/\text{collector} * 60 \text{ collectors} = 0.04458 \text{ m}^3$$

$$V_{\text{piping}} = \pi * (0.101905\text{m})^2 * (2 * 30\text{m} + 10\text{m}) = 0.0741 \text{ m}^3$$

$$V_{\text{pump}} = 0.000946 \text{ m}^3$$

$$V_{\text{heat exchanger}} = 0.41 \text{ m}^3$$

$$V_{\text{total}} = V_{\text{collectors}} + V_{\text{piping}} + V_{\text{pump}} + V_{\text{heat exchanger}} = 0.531 \text{ m}^3 \\ = 140 \text{ gallons}$$

$$P_{\text{initial}} = (0.4455 * 98.4 \text{ ft high}) + 10.3 \text{ psi} = 54.13 \text{ psi}$$

$$V_{\text{exp}} = V_{\text{total}} * 0.1 = 0.0531 \text{ m}^3 = 14 \text{ gallons}$$

$$V_{\text{vapor expansion}} = V_{\text{collectors}} = 0.04458 \text{ m}^3 = 11.77 \text{ gallons}$$

$$V_{\text{(expansion tank)}} = ((14 \text{ ga} + 11.77 \text{ ga}) \times (0.9 \times 87 + 14.5 \text{ psi})) / ((0.9 \times 87 - \\ 54.15 \text{ psi})) \\ = 98.94 \text{ gallons}$$

3.36 GLYCOL PUMP

A pump with variable flow rate was selected for pumping glycol to the roof and through the collectors. The chosen unit was selected based on its power rating, as well as range of flow rate capacity and viscosity tolerance. Pumping power was calculated using Equations 7-12 (Brown, 2000; Milnes, 2010). A list of variables can be found in Appendix D.

$$\text{Pumping power requirement} \quad P = \frac{\dot{m}gh}{3.6 \times 10^6} \quad (7)$$

Total head loss
$$h = h_f + z \quad (8)$$

Darcy-Weisbach Eq.
$$h_f = f \left(\frac{L}{D} \right) \left(\frac{v^2}{2g} \right) \quad (9)$$

Friction factor:
Laminar ($Re < 2000$)
$$f = \frac{64}{Re} \quad (10)$$

Blasius Eq: Turbulent,
hydraulically smooth
pipe friction factor
$$f = \frac{0.3164}{Re^{0.25}} \quad (11)$$

Reynolds number
$$Re = \frac{v\rho D}{\mu} \quad (12)$$

Where

- z is the approximate height of the building, estimated to be 24 at 3m per floor
- h is a function of head loss due to elevation and due to friction, h_f , throughout both the main glycol pipes and in the smaller pipes of each collector

Explanations for other variables can be found in Appendix D.

Pumping requirements were compared for corn-based glycol as well as ethylene glycol and are shown in Figure 11. The significant difference between the two heat transfer fluids is primarily due to the dynamic viscosity of corn glycol, which increases significantly as temperature decreases, while the ethylene glycol does not demonstrate such a trend (Cooling Tower Systems Inc., 2013; MEGlobal, 2008). In order to resist freezing the same extent as ethylene glycol, corn glycol must be mixed with water at a 60:40 ratio, rather than 50:50. This likely accentuates the difference in viscosity at lower temperatures.

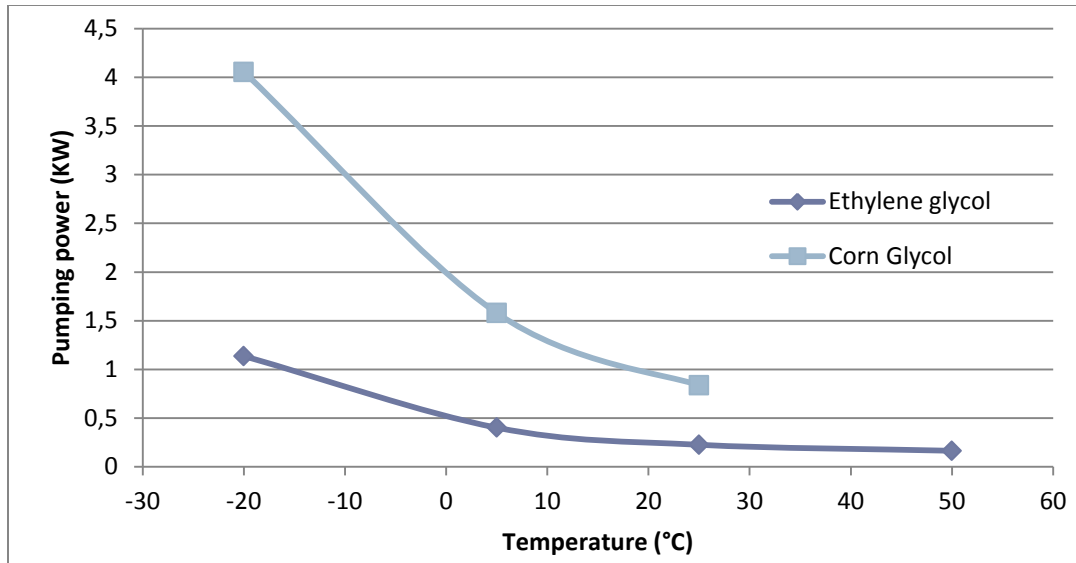


Figure 11: Comparison of pumping requirement for corn and ethylene glycols as a function of temperature

The pumping requirements are based on head loss that was calculated taking into account the two types of pipes present in the system. Their respective dimensions, flow velocity and more are indicated in Appendix D. Pipe lengths were determined using the simplified collector diagram that is also available in Appendix D, with the addition of a 2x24m for the distance from basement to roof. As mentioned in Section 3.2, each row of 12 panels is separated by 3 meters.

Due to the additional pumping requirement of corn glycol, it is recommended that ethylene glycol be used. Assuming glycol temperatures will not drop below -5°C , and considering a safety factor of 1.5, the pump should therefore have a power of at least 1.8 KW and be capable of sustaining flow between 4.8L/minute and 9.6 L/minute (AEE , 2009).

3.37 GLYCOL PIPES

A McGill Upper Residences plumber, Mr. Patterson, stated that the glycol pipes running from the basement to the roof and back can be up to approximately 1.25” in diameter. This would allow a 1”, or 2.54 cm, stainless steel pipe with 20mm of mineral wool insulation. Stainless steel is a common material used in solar thermal systems, due to its resistance to corrosion (Caleffi Hydronic Solutions, 2012). Mineral wool, also commonly used in pipe insulation is a preferred material due to its low average thermal conductivity of $0.04 \text{ W m}^{-1} \text{ K}^{-1}$ (SPI, 2011). These

materials are well suited to handle the corrosive heat transfer fluid, which may possibly reach temperatures of 80°C or more (AEE , 2009).

3.38 OTHER COMPONENTS

Check valves will be needed to prevent water from flowing backwards. For instance, between the heat exchanger and the storage tank, a check valve is needed to avoid hot water returning to the heat exchanger. A mixing valve is also needed in the proposed system as it will mix heated water with cold water from the municipal system, in order to prevent scalding.

Figure 12 is a diagram of the main components of the solar water heating system.

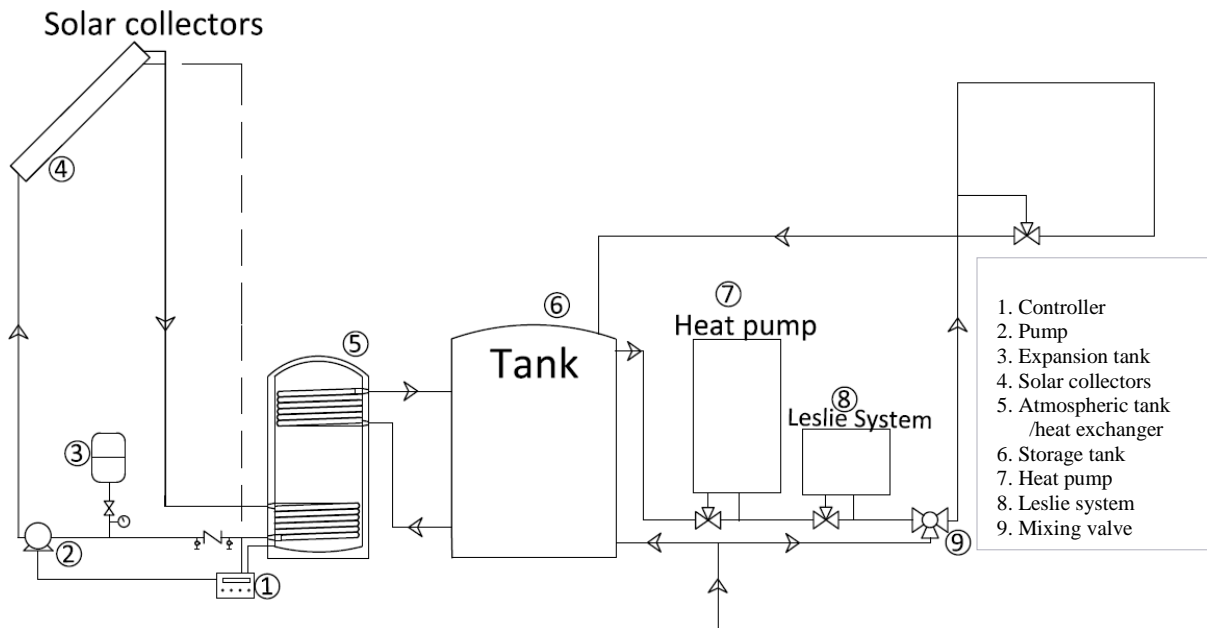


Figure 12: System component diagram

4. COMPUTATIONAL SYSTEM MODEL

Since the construction of a prototype for this project is prohibitively costly, a computational model of the heat transfer occurring throughout the McGill Upper Residences solar thermal system has instead been developed using the MATLAB Simulink software.

4.1 DESCRIPTION OF THE MODEL

4.1.1 PURPOSE

The model was set up with three primary objectives in mind:

1. Validation – Numerous parameters, such as glycol flow rates, pipe diameters, total panel area and inclination, estimated demand, size of heat exchanger, water storage tank volume and more had to be determined to include in the final deliverables of the project. The interaction of these multiple components is difficult to calculate analytically. The computational model was thus intended in part to run using these parameters, to see whether the results demonstrated “logical” answers that met expectations based on a review of similar systems. This is further discussed in Section 4.3.1.
2. Estimating heat loss along glycol pipes – Given the long distance that the glycol must run from roof to basement (24m), it was deemed important to quantify potential heat losses.
3. Sizing the heat pump – The heat pump sized in the context of Design 2 was only a preliminary number and could be better be estimated using a computational model that takes into account the many selected parameters and their interactions.

4.1.2 CONCEPT

The system is divided into 3 main blocks, as shown in Figure Figure 13: Diagram of the computational model broken down into 3 main blocks.

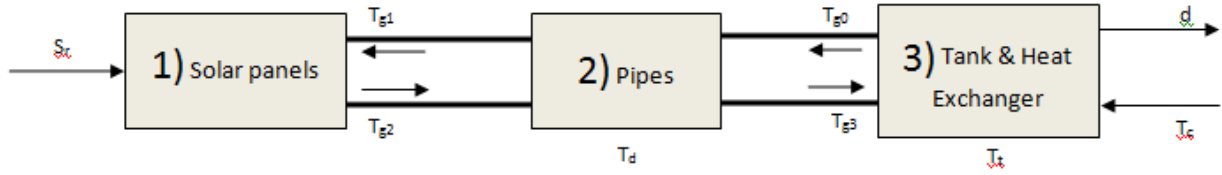


Figure 13: Diagram of the computational model broken down into 3 main blocks

4.1.2.1 SOLAR PANELS (BLOCK 1)

Energy transmitted to glycol is a function of several input parameters: solar irradiance (quantity and angle), ambient temperature, cloud cover, wind, glycol flow rate, collector type, collector area and more. In the case of the model, some of these parameters could not be taken into account as the system would become overly complex. Power input on the roof is thus represented by Equation (13), where variables and their units are listed in Appendix E.

Power input to heat transfer

$$q_{in} = n A_{aperture} S_r \quad (13)$$

Collector efficiency

$$n = n_0 - a_1 \left(\frac{T_m - T_a}{G} \right) - a_2 \left(\frac{(T_m - T_a)^2}{G} \right) \quad (14)$$

Glycol temperature differential at collector exit

$$dT_{g2} = \frac{q_{in}}{\dot{m}_g c_{pg}} dt \quad (15)$$

Average glycol temperature

$$T_m = \frac{1}{2} (T_{g2} + T_{g1}) \quad (16)$$

4.1.2.2 GLYCOL PIPES (BLOCK 2)

Temperature of glycol at points T_{g3} (entering heat exchanger) and T_{g1} (entering collectors) is a function of heat loss along the pipes. This is calculated based on the inner area of pipes for a better estimate of actual heat transfer and is seen in Equations (17)-(20) (Ghoshdastidar, 2004). Equations (21) and (22) demonstrate how the heat loss is then used to determine the change in glycol temperature at the end of the pipe section. Variables and their units are listed in Appendix E.

$$\text{General heat loss} \quad q_{loss} = UA_{gp,in}\Delta T \quad (17)$$

$$\text{Heat loss, roof to basement} \quad q_{loss23} = \left(\frac{1}{R_{eq}}\right)(2\pi r_i L_{gp})(T_{g2} - T_d) \quad (18)$$

$$\text{Heat loss, basement to roof} \quad q_{loss01} = \left(\frac{1}{R_{eq}}\right)(2\pi r_i L_{gp})(T_{g0} - T_d) \quad (19)$$

$$\text{Thermal resistance} \quad R_{eq} = \frac{1}{U} = \frac{1}{h_g} + \frac{r_i(\ln(r_o - r_i))}{k_{gp}} + \frac{r_i(\ln(r_{ins} - r_o))}{k_{ins}} + \frac{r_i}{h_{air}r_o} \quad (20)$$

$$dT_{g3} = \frac{q_{23}}{\dot{m}_g c_{pg}} dt \quad (21)$$

$$dT_{g1} = \frac{q_{01}}{\dot{m}_g c_{pg}} dt \quad (22)$$

4.1.2.3 STORAGE TANK AND HEAT EXCHANGER (BLOCK 3)

This block models heat transfer from glycol to water. First, energy transfer through heat exchanger is calculated, based on the temperature differential between glycol and water. This heat transfer value is equivalent to the energy loss from glycol passing through the heat exchanger and is thus used to calculate exiting glycol temperature, while the same change in energy is used to determine the temperature change of water tank. Demand, or hot water output,

is also used in determining change in tank temperature. Variables and their units are listed in Appendix E.

Heat transfer in heat exchanger

$$q_{hx} = q_{tank,in} = q_{loss3-0} = U_{i,hx} A_{hx,in} (T_{g3} - T_t) \quad (23)$$

Thermal resistance of heat exchanger

$$R_{eq,hx} = \frac{1}{U_{i,hx}} = \frac{1}{h_g} + \frac{r_{ihx}(\ln(r_{ohx} - r_{ihx}))}{k_{Cu}} + \frac{r_{ihx}}{h_w r_{ohx}} \quad (24)$$

Change in glycol temperature at hx exit

$$dT_{g0} = \frac{-q_{hx}}{\dot{m}_g c_{pg}} dt \quad (25)$$

Power out of tank

$$q_{tank,out} = \dot{m}_d c_{pw} (T_{tank} - T_c) \quad (26)$$

Change in overall tank energy

$$dQ_{tank} = q_{tank} = (q_{hx} - q_{tank,out}) dt \quad (27)$$

4.1.2.4 INITIAL CONDITIONS AND LIMITS

Initial temperatures were set in all fluids in order to more realistically model heat transfer in the system at any given time. Otherwise the system would require a start-up period, possibly of several days. The temperature of water in the tank and of the glycol both begin at 55°C.

4.3 RESULTS

In order to test the functionality of the system, simulations were run in parallel for three scenarios of power input and hot water demand. The run time was 72 hours, with 1-hour intervals. The scenarios can roughly be described as follows and the first 24 hours of each one can be found in Appendix E:

1. Best case scenario: Sunny day in July (maximum irradiance) and occupancy of 5 people.

2. Average scenario: Sunny day in June (high irradiance) and occupancy of 50 people, greatest consumption in the morning, but demand is relatively steady with peaks of no more than 20% of the total daily consumption.
3. Worst case scenario: Cloudy day in May, resulting in a 50% reduction in available power (Igweonu, 2011). Maximum occupancy at 110 people, with large peaks at concentrated and inopportune times, such as early morning and late evening.

Solar irradiation was based on the monthly average, total aperture area, number of useful sunlight hours and estimated reduction in available power due to cloud cover. Average irradiation data for a 19° panel tilt in Montreal was obtained from RETScreen, software provided by the Canadian government, and is shown in Table 5 - Average irradiance data for Montreal (RETScreen). Demand was based on number of occupants, estimates of average daily and peak hour consumption and the timing of hot water usage.

Table 5 - Average irradiance data for Montreal (RETScreen)

Month	Useful sunlight (h d ⁻¹)	Irradiance (KWh m ⁻² d ⁻¹)
May	7.42	5.43
June	8.20	5.74
July	8.84	5.88
Aug	7.74	5.07

4.3.1 VALIDATION OF SELECTED PARAMETERS

Since the selection of parameters detailed in Section 3 is based on a wide range of literature, the model played an important role, confirming that these could in fact interact as expected. For instance, Section 4.3.2 will show how glycol pipe and insulation materials affect heat transfer over time and Section 4.3.3 demonstrates that under various scenarios, tank temperature varies more or less as expected.

The model was useful in confirming facts that may have been somewhat ambiguous in the literature. For instance, in large-scale systems many design guides recommend an average glycol flow rate of 5-20 kg m⁻² h⁻¹ (AEE , 2009). However, none are clear on whether the panels are configured in series, in parallel or both. If set up in parallel, the flow rate in each collector is decreased. There was a concern, therefore that the design guidelines had been misunderstood. However, the results of the model, shown in Figure 16, confirm that this is a sufficient rate.

4.3.2 COMPARISON OF INSULATED AND NON-INSULATED PIPES

The integrated results of hourly temperature decrease in glycol running through pipes from the roof to the basement show an accumulated temperature loss of 60°C for non-insulated pipes over the 72-hour simulation period. In contrast, the insulated pipes show a total loss of only 12°C. The accumulated temperature changes represent losses of 5.33e6 and 1.00e6 J h⁻¹.

At an average Montreal radiation for the month of June that is 5.74kWh/m²/day, with a 144m² panel area and solar period of roughly 8.20 hours, the hourly radiation is therefore 3.62e8 J/h. Given average collector efficiencies of roughly 0.43%, energy uptake by solar panels is approximately 1.59e8 J h⁻¹. Losses without and with insulation would therefore represent, respectively, 3.34% and 0.62% of incoming energy.

Over the course of a 4-month summer, approximately 2880 hours, losses are therefore 4264 KWh and 800 KWh. At approximately \$0.06 per KWh this is equivalent to a monetary loss of 256\$ per summer, compared to 48\$ (Parr, Feb 2012). Of course if the system is intended to last over 20 years, these losses increase to \$117.00 compared to \$960.00. Actual losses are likely to be somewhat higher given that the system will run as an auxiliary power source for water heating for the remaining 8 months of the year and thus the need for insulation would be even greater.

Observed cumulative heat losses obtained from simulations are shown in Figures Figure 14 and Figure 15.

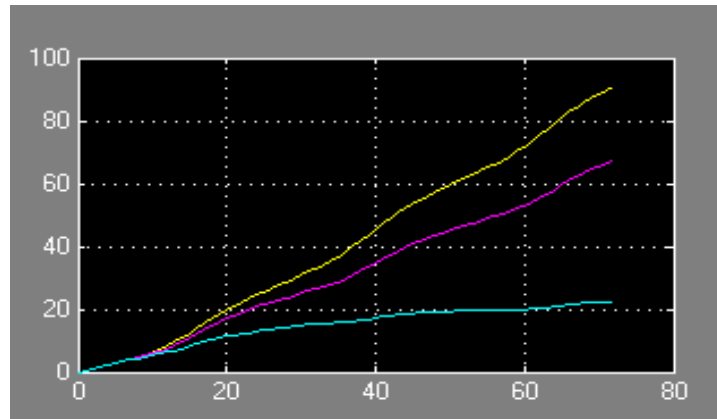


Figure 14: Accumulated Heat Loss (deg. C) in non-insulated glycol pipes over 72 hours

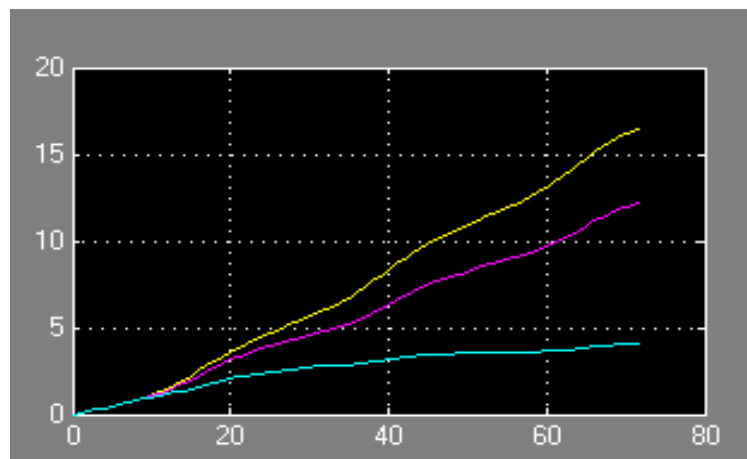


Figure 15: Accumulated Heat Loss (deg. C) in insulated glycol pipes over 72 hours

4.3.3 SIZING THE HEAT PUMP

Since it acts as a backup heat source, in the event that solar input is insufficient to meet the demand, the heat pump must be sized for the worst-case scenario. In this scenario, results of the simulations show that a peak demand of 1254 L is required when the tank is at only 22°C. The third day, in which the tank temperature drops just below 20°C, is not taken into account because of model limitations that will be discussed shortly. The quantity and timing of demand used for simulations can be found in Appendix E.

The heat pump must therefore be capable of heating 1254 L of water from 22°C to 60°C in one hour. It has a small built-in storage tank, which is maintained at 60°C. In this case, the heat pump

would only need to a first-hour-rating that is sufficiently high to heat a water mass equivalent to the difference between the required energy supplement and the energy within the heat pump's storage tank.

The third day was not included, as the model has limitations that lead it to be very conservative in estimating heat pump capacity. This is because the model assumes perfect mixing in the near 6000 L water storage tank. However, thermal stratification in hot water tanks will significantly increase performance, as solar energy is concentrated in the upper section of the tank by natural convection, rather than being distributed throughout. In the selected tank, the 1245 L demand would therefore pull only from the top 25% of the tank and would thus be likely to draw water that is significantly warmer than the observed 22°C. In the event that this solar thermal system were to be implemented, thermal stratification would need to be taken into account in order to avoid selecting an overly large heat pump. Results of the 3-scenario simulation are shown in Figure 16.

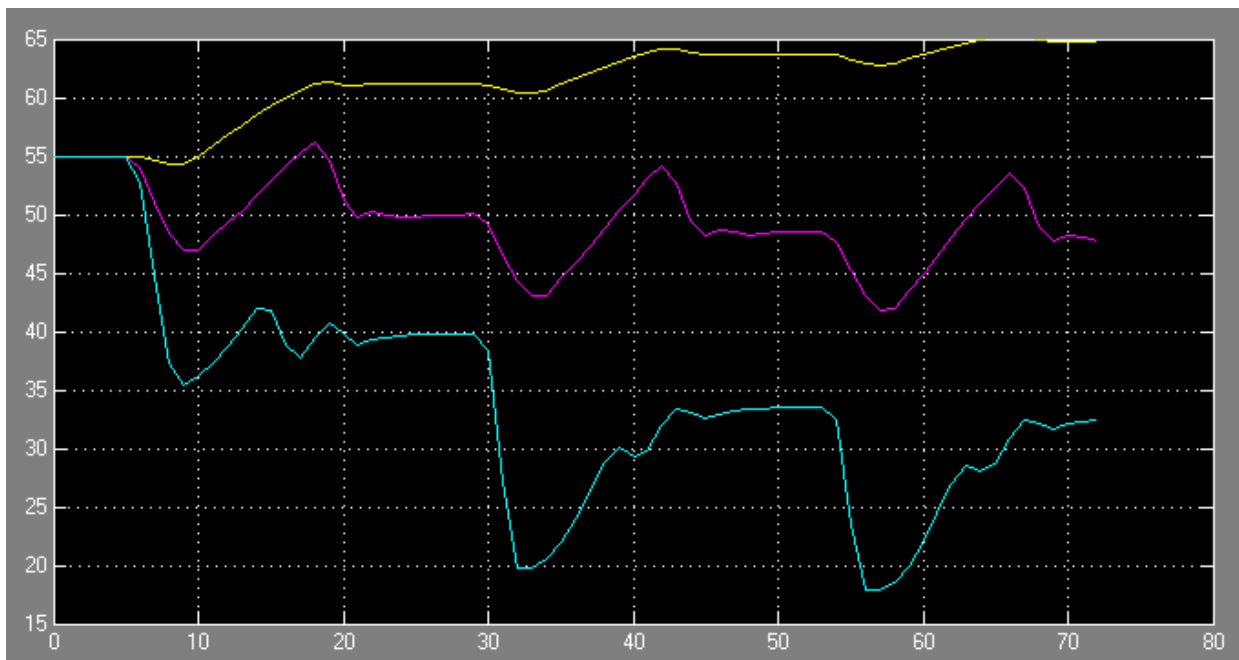


Figure 16: Results of simulation with best (yellow), medium (violet) and worst-case (blue) scenarios show tank temperature (deg. C) over time (hrs)

5. RISK AND FAILURE ANALYSIS

5.1 MODEL REACTION TO EXTREME SCENARIOS

As mentioned previously, the model was run at irradiance and demand extremes for the summer season in order to observe reactions in glycol and tank temperatures. Scenario 1, shown in Figure 166 (in yellow), demonstrates the need for a control system, as specified in Section 3. Without this, the tank temperature

-results = sunny extreme problematic temp increase in tank bc model has fixed flow rate, bad extreme is problematic because perfect mixing in tank had to be assumed

5.2 COMPONENT FAILURE

The risk of solar collector failure is low, since collectors are made from durable materials and leaks would more likely be caused by deficient pipe fittings.

As previously stated, the heat exchanger and coils should last 20-25 years, since the tank has few components. In order to ensure longevity, the water in the tank should be changed every 6 or 7 years. Bacterial growth will be inhibited by high water temperatures if the system functions as designed (EcoSolaris, 2013).

Failure of the pump could lead to critical damage on days when radiation is high if it is not repaired in a timely fashion, since the heat transfer fluid will overheat and quickly degrade.

The controller and the temperature sensors ensure the optimal flow rate of the heat transfer fluid from the collectors to the heat exchanger. The failure of one of these components can lead to the inability of the pump to stop glycol circulation when the heat transfer fluid temperature is lower than that of the water at the bottom of the heat exchanger, resulting in cooling of stored water. Moreover, if the solar collectors are not properly grounded, a storm may interfere with or even damage the controller. Proper grounding should thus be installed for the solar collectors.

The expansion tank is important to protect the system and proper sizing is crucial. Incorrect sizing of this unit can result in undesirably high pressures in the system, valve breakage and other problems.

The boiling point and pH of the glycol should be tested every year and changed every 5 years, as long as the expansion tank runs properly. Otherwise, glycol may need to be changed earlier. Even though heat transfer fluids are designed to have high flash points and high combustion points, they are still flammable when heated at high temperatures.

5.3 ROOFTOP CONCERNS

There are significant risks associated with mounting collector panels on the roof, particularly when using a ballast system rather than a support structure which is bolted down. Unexpected winds which exceed velocities which the system is designed for could cause collectors to tip, slide or fly. The consequences could range from component damage or destruction, to having collectors fall from the rooftop injuring, or possibly killing pedestrians below. As can be seen in the load calculations portion of the Section 3, the system has been designed for wind pressures with a frequency of 1/30 years which is greater than the lifespan of the system. It conservatively assumes unobstructed gusts, which will never occur on the roof since the panels effectively block wind for each other, and those at the edges will experience a decreased pressure due to “ground friction” since they are low structures (relative to the rooftop) (McKyes, 2013). Additionally, the ballast required to prevent sliding has been exceeded by 50% (safety factor of 1.5) in order to provide additional safety. Further measures could be taken which would require additional work and funds, including, but not limited to, installation of roof parapets, implementation of a bolted support system, or use of deflectors to reduce lift and increase load. Ultimately it is up to the discretion of a professional engineer and the client to determine the degree of precaution which should be taken. When comparing the calculated total load incurred by the collectors to the roof load capacity, the following should be taken into consideration: the maximum snow load should be subtracted from the roof load capacity, and an additional safety factor should be subtracted in order to accommodate the weight of workers and equipment required for collector installation and maintenance, as well as the relatively negligible weight of the additional glycol pipes, which will run between the collectors.

5.4 ECONOMICS OF RISK

All system selections were made based on a risk vs. cost analysis. While the goal of the client is to minimize costs, project decisions must also be made in order to ensure that the energy demands will be met under the most difficult possible conditions and that the design meets standard safety codes.

6. OPTIMIZATION & RECOMMENDATIONS

The entire design process was a repeating cycle of analysis and calculation, testing and optimization. Improvements to the project were thus made throughout, resulting in the decisions that are highlighted in Section 3: Engineering Analysis and Design Specifications. The following section thus recalls some of the major optimizations that occurred throughout the semester, as well as recommendations for future design improvements.

6.1 ROOF CONSIDERATIONS

The results of the wind and snow load calculations show that the use of a ballast system with panels at angles of 19 and 69 degrees will incur enormous loads on the roof structure. The client should compare these values to the roof load capacity with the portion allocated for snow load, maintenance staff, and equipment removed, to determine if such loads could be supported. If not, it is recommended that the system be bolted into the rooftop rather than ballasted. Alternatively, the winter angle could be reduced since the optimal 69 degree tilt results in extreme drag conditions that drastically increase the required ballast weight per collector. Additionally, deflectors mounted on the North side of the collectors could be used to reduce lift and consequently ballast weight.

The design recommended here was created with the goal of maximizing the potential energy savings generated by the system through optimal collector tilt year-round. However, such a system would require maintenance staff to change the angles twice a year, as well as may require the use of custom-built collector supports with adjustable angles. Both of these factors will increase system costs, and should be considered when the client is assessing the impact of their final budget. Alternatively, a system with an angle of 45-55 degrees could be used year-round to eliminate these concerns, with relatively small reductions in energy harvest.

6.2 SYSTEM COMPONENTS

Components have been primarily chosen to meet the hot water consumption demand for the summer months. However, the implementation of the solar water heating system coupled with the heat pump is conditional to the space available in the basement and optimal dimensions of

every component have been chosen as their dimensions can vary. The components that have been described in this report are recommended but various configurations are possible.

6.3 THE COMPUTATIONAL MODEL

The model was optimized throughout the semester, adding complexities to the system as it was developed. It first began with an input of constant solar radiation per second and zero demand. A constant demand per second was then added. The use of the “per second” interval facilitated unit conversion, as many variables were measured in terms of joules or watts (J s^{-1}). Once results from these simulations were validated and verified, a gain block representing the time interval, dt , was integrated throughout the model to allow hourly observations of heat transfer. An equation for panel efficiency was also added to take into account the impact of variations in glycol temperature. The three simulation scenarios were then constructed and imported from Excel, to test the model in various irradiation and demand contexts.

Despite this progress, some important limitations remain. The most crucial are the lack of a control system for glycol flow rates and the assumption of perfect mixing in the water tank.

It would not be overly complicated to implement an if/else block that bases its actions on temperature differentials between temperature in the water storage tank and of the glycol on the roof. The block could initially have ability to simply stop or start flow and could be developed to provide a small range of flow rates. This would reduce heat loss during periods of non-useful radiation and at night, while improving efficiency in the event of high radiation.

More importantly, modeling thermal stratification in the water storage tank would significantly increase output water temperatures, as peaks draw only about 25% of the tank volume. This is because the demand is fed from the top portion of the tank, which contains warmer water, due to natural convection. The topic of computer modeling for thermal stratification is the focus of many research papers that are available online. Multiple methods exist, though the node method seems most applicable for use with Simulink.

In short, further development of the model would lead to more realistic and thus more useful results and avoid overdesign of the solar thermal water heating system.

FINAL REMARKS

Overall, the deliverables generated over the last two semesters have effectively assessed the feasibility of a solar thermal system to heat water during the summer in the McGill Upper Residences. The team's recent presentation to the client was received with much satisfaction and positive feedback. The final report will be kept for future reference when the need becomes more urgent and funding for such a project becomes available.

REFERENCES

AEE . (2009). *Thermal use of solar energy*. Retrieved 10 2012, from Solar thermal systems and components: <http://fr.scribd.com/doc/52225551/16/CPC-Collector>

Alternative Energy Tutorials. (2012, 11). *Flat plate collector* . Retrieved 11 03, 2012, from Alternative energy tutorials: <http://www.alternative-energy-tutorials.com/solar-hot-water/flat-plate-collector.html>

AO Smith. (2012, October). *Commercial storage tank*. Retrieved April 5, 2013, from Hot Water Canada: (<http://www.hotwatercanada.ca/spec/storage/aostt35400.pdf>)

Aps. (2004). *Vertical Atmospheric storage tanks*. Retrieved April 16, 2013, from APS water: <http://www.apswater.com/shopdisplayproducts.asp?id=753&cat=Vertical-Atmospheric-Storage-Tanks>

Bosch. (2011, June). *Solar Thermal Expansion Tank Sizing Guide*. Retrieved April 15, 2013, from Bosch: http://www.bosch-climate.us/files/201107252223380.SOLAR_Expansion_Tank_Sizing_Bulletin.pdf

Brown, G. (2000, June 22). *The Darcy-Weisbach Equation*. Oklahoma, USA: Oklahoma State University. Retrieved March 10, 2013, from <http://biosystems.okstate.edu/darcy/DarcyWeisbach/Darcy-WeisbachEq.htm>

Caleffi Hydronic Solutions. (2012). *Components for Solar Thermal Systems*. Italy. Retrieved February 1, 2013, from http://www.caleffi.com/en_IT/caleffi/Files/giudes/files/03117_en.pdf

Calpak Solar Thermal. (n.d.). *Collector model comparison chart*. Retrieved April 2013, from Clean Power Solar Thermal: <http://www.cpsolarthermal.com/products/collector-comparison-charts/>

Cash Acme. (2006, November). *T and TV Series Expansion Tanks* . Retrieved April 10, 2013, from Cash Acme: http://www.cashacme.com/_images/pdf_downloads/products/expansion_tanks/t_series/TSeries_Spec.pdf

- Cooling Tower Systems Inc. (2013). Introducing Biodegradable Corn Glycol. Macon, Georgia, USA. Retrieved March 15, 2013, from http://www.coolingtowersystems.com/corn_glycol.php
- EcoSolaris. (2013). *Solar water heating installation in Quebec*. Retrieved March 15, 2013, from Les entreprises écoSolaris: <http://www.ecosolaris.ca/en/solar-heating-system-quebec.php>
- Gaisma. (n.d.). *Montreal, Canada - Sunrise, sunset, dawn and dusk times, table*. Retrieved April 2013, from <http://www.gaisma.com/en/location/montreal.html>
- Ghoshdastidar, P. S. (2004). *Heat Transfer*. Oxford, UK: Oxford University Press.
- Igweonu, E. I. (2011). Solar Collector Efficiency: Analysis and Application. *Continental Journal of Engineering Sciences* , 24-30.
- Kalogiro, S. A. (2009). Solar Water Heating Systems. In S. A. Kalogiro, *Solar Energy Engineering: Processes and systems*. Academic Press.
- McKyes, Edward, Dr. "Wind Loads on Solar Collectors." Personal interview. 2013.
- MEGlobal. (2008). Ethylene Glycol Product Guide. Alberta, Canada. Retrieved March 15, 2013, from http://www.meglobal.biz/media/product_guides/MEGlobal_MEG.pdf
- Milnes, M. (2010). *The Mathematics of Pumping Water*. London, UK: The Royal Academy of Engineering. Retrieved March 10, 2013, from http://www.raeng.org.uk/education/diploma/maths/pdf/exemplars_advanced/17_pumping_water.pdf
- National Building Code of Canada, 2010*. Vol. 2. [Ottawa, Ont.]: National Research Council Canada, Institute for Research in Construction, 2010. Print.
- Parr, F. (Feb 2012). *Energy consumption report 2006-2011*. Montreal: McGill University services, Utilities and Energy Management.
- Patterson, R. (2012, 09 24). McGill University Plumber. (B. E. Team, Interviewer) Montreal, Quebec, Canada.

Solar Hot USA. (2009). *Solar hot water storage tanks*. Retrieved March 15, 2013, from Solar Hot Usa: <http://www.solarhotusa.com/products/solar-tanks.html>

SPI. (2011, September). Mineral Wool Pipe Insulation. Lancaster, Pennsylvania, USA: Specialty Products & Installation. Retrieved February 1, 2013, from http://www.programs.insulation.org/Scripts/4Disapi.dll/4DACTION/WebFile/Mineral_Wool_Pipe_Insulation.pdf?action=Category&Category=MTL&WFID_W=117&Time=18876596&MenuKey=234

Solar for Flat Roofs and Ground Mounting. Viridian Solar, 2013. Web. 17 Apr. 2013. <http://www.viridiansolar.co.uk/Products_Solar_Panels_for_Flat_Roof_Installation.htm>.

Standard Block. Boral Best Block, 2013. Web. 17 Apr. 2013. <<http://www.boralbestblock.com/product-lines/masonry/standard-block>>.

Time and date. (2012). *Sunrise and sunset in Montreal*. Retrieved 10 10, 2012, from [timeanddate.com](http://www.timeanddate.com): <http://www.timeanddate.com/worldclock/astronomy.html?n=165&month=12&year=2012&obj=sun&af1=-11&day=1>

UK Copper Board. (2010). *Copper Solar Thermal systems*. Retrieved March 19, 2013, from UK copper board: <http://www.copperinfo.co.uk/plumbing-heating-and-sprinklers/downloads/pub-827-copper-solar-thermal-systems.pdf>

US Department of Energy. (2003, 12). *Energy Efficiency and Renewable Energy*. Retrieved 10 2012, from Heat your water with the sun: <http://www.nrel.gov/docs/fy04osti/34279.pdf>

APPENDIX

APPENDIX A – ROOF LOAD

According to the National Building Code of Canada (2010),

The basic roof snow load equation is:

$$S = I_s * (S_s * (C_b * C_w * C_s * C_a) + S_r)$$

I_s is the importance factor to be used with snow load. As with wind load there is an importance factor to be used with Ultimate Limit State (ULS) for strength design and another to be used with the Serviceability Limit State (SLS) for deflection design.

Building Importance Category	ULS I_s (Strength)	SLS I_s (Deflection)
Normal Importance	1.0	0.9
High Importance	1.15	0.9
Post Disaster	1.25	0.9

Table 4 – Snow importance factors

S_s and S_r are the snow and rain parameters set by the building authority and under NBCC 2005 are based on a return period of 50 years.

S – specific loading (kPa)

I_f – importance factor

S_s – ground snow load (kPa) from Building Code site-specific climate data

C_b – the basic roof snow load multiplier. $C_b=0.8$ for small roofs (maximum dimension less than 70m).

C_w – wind exposure factor

Normal = 1.0

Exposed to wind on all side =0.75

North of tree line =0.5

C_s – slope factor 1 for roof slopes less than 15 degree regardless of the roof being slippery or not. Above this slope there are variations depending on whether the slope is classed as being slippery or not. For slippery roofs $C_s=0$ at 60 while for nonslippery roofs $C_s=0.0$ when the roof slope exceeds 70 degree, a value of $C_s=0$ means that the Code considers that there is no snow on the roof. C_a – accumulation factor = 1.0

S_r – rain load from Building Code site-specific climate data

From the building blueprints provided by the client we know that the roof has the following dimensions (ignoring the raised facilities room on top which will not have collectors on it).

$$l = 54.65\text{m}$$

$$w = 14.8 \text{ m}$$

The formula for the characteristic length which determines if the roof is classified as large or small is as follows:

$$l_c = 2w - w^2/l = 29.6\text{m} - 4.008\text{m} = 25.6\text{m}$$

Since 25.6 m is less than 70m the roof is classified as “small”. According to the 2010 code, $C_b = 0.8$ for small roofs.

APPENDIX B: COMPARISON OF TILT ANGLES FOR SOLAR COLLECTORS

Table B1: Energy collected from panels with winter tilt of 69°

	kWh/ m ² /d	Collector efficiency	Net kWh /m ² /d	Collector Area	kWh/ d
annual	3,61	0,4	1,444	145	207,9
Jan	3,26	0,4	1,304	145	187,8
Feb	4,29	0,4	1,716	145	247,1
Mar	4,48	0,4	1,792	145	258,0
Apr	3,92	0,4	1,568	145	225,8
May	3,96	0,4	1,584	145	228,1
Jun	3,95	0,4	1,58	145	227,5
Jul	4,14	0,4	1,656	145	238,5
Aug	3,98	0,4	1,592	145	229,2
Sep	3,87	0,4	1,548	145	222,9
Oct	3,11	0,4	1,244	145	179,1
Nov	2,09	0,4	0,836	145	120,4
Dec	2,33	0,4	0,932	145	134,2

Table B2: Energy collected from panels with summer tilt of 19°

	kWh/ m ² /d	Collector efficiency	Net kWh /m ² /d	Collector Area	kWh/ d
annual	3,92	0,4	1,568	145	225,8
Jan	2,24	0,4	0,896	145	129,0
Feb	3,27	0,4	1,308	145	188,4
Mar	4,24	0,4	1,696	145	244,2
Apr	4,74	0,4	1,896	145	273,0
May	5,43	0,4	2,172	145	312,8
Jun	5,74	0,4	2,296	145	330,6
Jul	5,88	0,4	2,352	145	338,7
Aug	5,07	0,4	2,028	145	292,0
Sep	4,22	0,4	1,688	145	243,1
Oct	2,85	0,4	1,14	145	164,2
Nov	1,71	0,4	0,684	145	98,5
Dec	1,61	0,4	0,644	145	92,7

APPENDIX C: COLLECTOR EFFICIENCIES

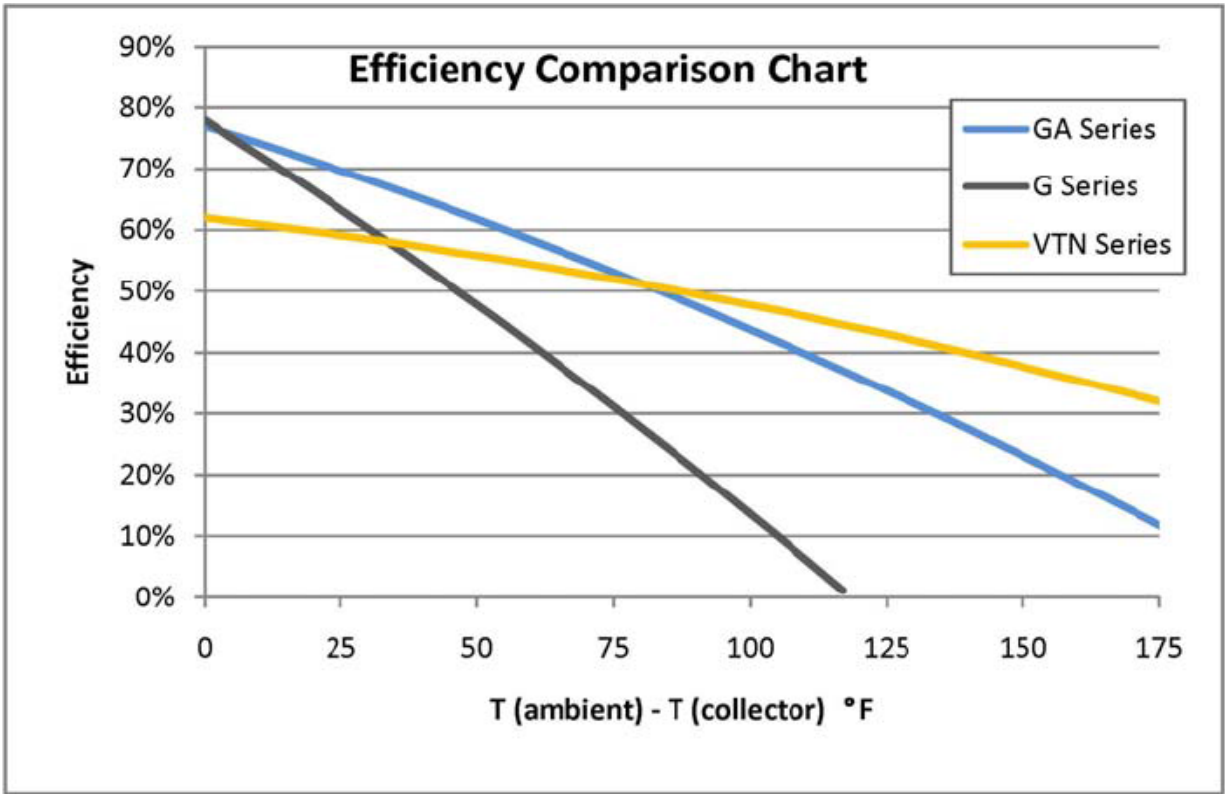


Figure 17: Comparison of Panel Efficiencies (Calpak)

APPENDIX D: PUMPING POWER CALCULATIONS

Table 6 - Parameters used to calculate head loss throughout the glycol loop, based on both main glycol pipes and pipes in collectors

Pipes	Units	Ethylene glycol	Corn glycol
Main glycol pipe			
Diameter	m	0.01905	0.01905
Area	m ²	0.000285023	0.000285023
Flow rate	kg/s	0.4	0.4
Flow velocity (avg)	m/s	1.328218557	1.32771592
Length (m)	m	84.84	84.84
Hf/f	m	400.4476634	400.1446384
Pipes in collectors			
Diameter	m	0.00635	0.00635
Area	m ²	3.16692E-05	3.16692E-05
Flow rate	kg/s	0.008	0.008
Flow velocity (avg)	m/s	0.23907934	0.238988866
Length (m)	m	640.08	640.08
Hf/f	m	293.6605626	293.438345

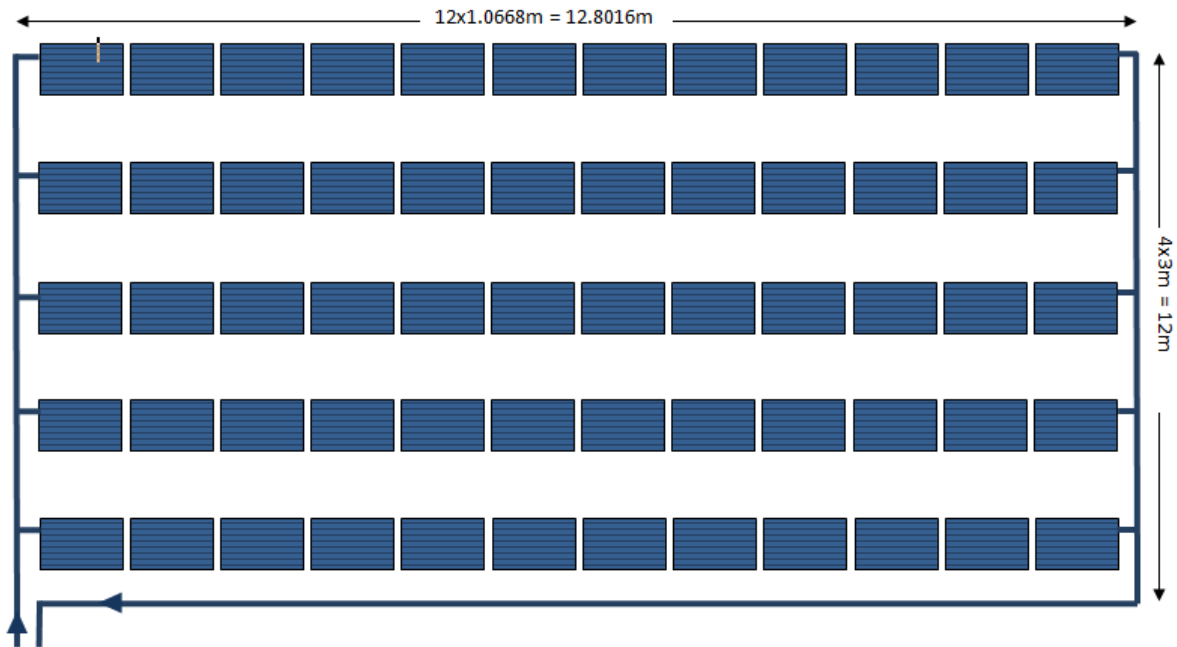


Figure 18 - Simplified schematic of piping distances on the roof

Total pipe lengths in the glycol loop were determined based on the Figure 18 and are broken down in Equations (7) (main pipe) and (8) (pipes in collectors). There are 10 pipes running through each of the 60 collectors.

$$L = (24m \times 2) + 2(3m \times 4) + (1.0668m \times 12) = 84.84m \quad (7)$$

$$L = 1.0668m \times 10 \times 60 = 640.08m \quad (8)$$

List of variables for pumping power calculations

P: pumping power (KW)

***m*:** glycol flow rate (1440 kg h⁻¹)

g: gravitational acceleration (9.81 m s²)

h: total head loss (m)

hf: head loss due to friction (m)

z: elevation to be overcome by pump (24m)

f: friction factor

Re: Reynolds number

L: length of glycol pipes (m)

D: diameter of glycol pipes (m)

v: velocity of glycol in pipe (m s^{-1})

μ : dynamic viscosity ($\text{kg m}^{-1} \text{s}^{-1}$)

ρ : density of glycol-water mixture (kg m^{-3})

LIST OF VARIABLES USED IN THE COMPUTATIONAL MODEL
CALCULATIONS

\dot{m} : glycol flow rate (kg s^{-1})

a_1, a_2 : coefficients for collector efficiency calculation

A_{aperture} : area of collector pipes exposed to sunlight (m^2)

c_{pg} : specific heat capacity of glycol ($\text{J kg}^{-1} \text{C}^{-1}$)

c_{pg} : specific heat capacity of water ($\text{J kg}^{-1} \text{C}^{-1}$)

c_{pw} : specific heat capacity of water ($\text{J kg}^{-1} \text{C}^{-1}$)

G : average solar radiation for May-August ($\text{J s}^{-1} \text{m}^{-2}$)

h_{air} : heat transfer coefficient of air ($\text{W m}^{-1} \text{C}^{-1}$)

h_{gp} : heat transfer coefficient of glycol ($\text{W m}^{-1} \text{C}^{-1}$)

K_{Cu} : heat transfer coefficient of heat exchanger coils, copper ($\text{W m}^{-1} \text{K}^{-1}$)

K_{gp} : heat transfer coefficient of glycol pipes ($\text{W m}^{-1} \text{K}^{-1}$)

K_{ins} : heat transfer coefficient of glycol pipe insulation, mineral wool ($\text{W m}^{-1} \text{K}^{-1}$)

L_{gp} : length of single basement to roof glycol pipe (m)

n : actual efficiency of solar collector

n_0 : ideal efficiency of solar collector

q_{01} : heat loss along glycol pipe from heat exchanger to roof (J h^{-1})

q_{23} : heat loss along glycol pipe from collectors to heat exchanger (J h^{-1})

q_{hx} : power transmitted through heat exchanger (J h^{-1})

q_{in} : power transmitted to glycol on roof (J h^{-1})

$q_{\text{tank,out}}$: power out of tank, due to demand (J h^{-1})

R_{eq} : thermal resistance ($\text{m}^2 \text{C W}^{-1}$)

r_i : inner diameter of glycol pipes (m)

r_o: outer diameter of glycol pipes (m)

S_r: hourly solar radiation (J h⁻¹ m⁻²)

T_{amb}: ambient temperature on roof (°C)

T_c: temperature of city water entering tank/heat exchanger (°C)

T_d: temperature of ducts for glycol pipes (°C)

T_{g0}: temperature of glycol entering heat exchanger (°C)

T_{g0}: temperature of glycol exiting heat exchanger (°C)

T_{g0}: temperature of glycol exiting solar panels (°C)

T_{g1}: temperature of glycol entering solar panels (°C)

T_m: average glycol temperature throughout the collectors (°C)

T_t: temperature in solar storage tank (°C)

U: overall heat transfer coefficient (W m⁻² C⁻¹)

SCENARIOS FOR SIMULATION

Time (h)	Scenario 1		Scenario 2		Scenario 3	
	Best rad (J h ⁻¹ m ⁻²)	Best dem (m ³)	Med rad (J h ⁻¹ m ⁻²)	Med dem (m ³)	Worst rad (J h ⁻¹ m ⁻²)	Worst dem (m ³)
1	0	0	0	0	0	0
2	0	0	0	0	0	0
3	0	0	0	0	0	0
4	0	0	0	0	0	0
5	0	0	0	0	0	0
6	0	0.0285	0	0.285	0	0.627
7	0	0.057	0	0.57	0	1.94
8	0	0.0285	0	0.285	0	1.254
9	2248134.307	0.0285	504000	0.285	0	0
10	2634411.679	0	2520000	0	764921.7391	0
11	2634411.679	0	2520000	0	1317365.217	0
12	2634411.679	0.01425	2520000	0.1425	1317365.217	0

13	2634411.679	0	2520000	0	1317365.217	0
14	2634411.679	0	2520000	0	1317365.217	0
15	2634411.679	0	2520000	0	1317365.217	0.627
16	2634411.679	0	2520000	0	1317365.217	1.254
17	2634411.679	0	2520000	0	1317365.217	0
18	0	0	0	0	0	0
19	0	0.057	0	0.57	0	0
20	0	0.057	0	0.57	0	0.627
21	0	0	0	0	0	0
22	0	0	0	0	0	0
23	0	0.01425	0	0.1425	0	0
24	0	0	0	0	0	0

Figure 19: Scenarios for computer model simulations

TO VIEW THE MODEL

To view the model please see attached Simulink and .mat files, as well as the Excel document “MATLAB parameter names for Simulink”.